

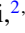



## Fundamental limitations in Lindblad descriptions of systems weakly coupled to baths

Devashish Tupkary <sup>1,2,3,\*</sup>, Abhishek Dhar <sup>2,†</sup>, Manas Kulkarni <sup>2,‡</sup> and Archak Purkayastha <sup>4,§</sup>

<sup>1</sup>Indian Institute of Science, Bangalore 560012, India

<sup>2</sup>International Centre for Theoretical Sciences, Tata Institute of Fundamental Research, Bangalore 560089, India

<sup>3</sup>Institute for Quantum Computing and Department of Physics and Astronomy,  
University of Waterloo, Waterloo, Ontario, Canada N2L 3G1

<sup>4</sup>School of Physics, Trinity College Dublin, College Green, Dublin 2, Ireland



(Received 12 July 2021; accepted 25 February 2022; published 16 March 2022)

It is very common in the literature to write a Markovian quantum master equation in Lindblad form to describe a system with multiple degrees of freedom and weakly connected to multiple thermal baths which can, in general, be at different temperatures and chemical potentials. However, the microscopically derived quantum master equation up to leading order in a system-bath coupling is of the so-called Redfield form, which is known to not preserve complete positivity in most cases. Additional approximations to the Redfield equation are required to obtain a Lindblad form. We lay down some fundamental requirements for any further approximations to the Redfield equation, which, if violated, leads to physical inconsistencies such as inaccuracies in the leading order populations and coherences in the energy eigenbasis, violation of thermalization, and violation of local conservation laws at the nonequilibrium steady state. We argue that one or more of these conditions will generically be violated in all the weak system-bath-coupling Lindblad descriptions existing in the literature to our knowledge. As an example, we study the recently derived universal Lindblad equation and use these conditions to show the violation of local conservation laws due to inaccurate coherences but accurate populations in the energy eigenbasis. Finally, we exemplify our analytical results numerically in an interacting open quantum spin system.

DOI: [10.1103/PhysRevA.105.032208](https://doi.org/10.1103/PhysRevA.105.032208)

### I. INTRODUCTION

A fundamental problem relevant across a wide range of fields including quantum optics [1], thermodynamics [2], chemistry [3], engineering [4], and biology [5] is to describe a quantum system with multiple degrees of freedom connected to multiple thermal baths. An approach very often taken is to derive an effective quantum master equation (QME) for the dynamics of the system assuming weak coupling between the system and the baths. The dynamics of the quantum system, as described by the QME, is often desired to be Markovian. It was shown by Gorini, Kossakowski, Sudarshan [6], and Lindblad [7] (GKSL) that a QME that preserves all properties of the density matrix and describes Markovian dynamics has to be of the form

$$\frac{\partial \hat{\rho}}{\partial t} = i[\hat{\rho}, \hat{H}_S] + \hat{\mathcal{L}}(\hat{\rho}),$$

$$\hat{\mathcal{L}}(\hat{\rho}) = i[\hat{\rho}, \hat{H}_{LS}] + \sum_{\lambda=1}^{D^2-1} \gamma_{\lambda} \left( \hat{L}_{\lambda} \hat{\rho} \hat{L}_{\lambda}^{\dagger} - \frac{1}{2} \{ \hat{L}_{\lambda}^{\dagger} \hat{L}_{\lambda}, \hat{\rho} \} \right), \quad (1)$$

which is commonly called a Lindblad equation. Here,  $\hat{\rho}$  is the density matrix of the system,  $\hat{H}_S$  is the system Hamiltonian,

$\hat{H}_{LS}$  is the Hermitian contribution due to the presence of the baths, commonly called the Lamb shift term,  $\hat{L}_{\lambda}$  are the Lindblad operators and  $\gamma_{\lambda}$  are the rates, and  $D$  is the dimension of the Hilbert space. Here we will confine our study to (effective) finite-dimensional systems. Both  $\hat{H}_{LS}$  and  $\hat{L}_{\lambda}$  are operators in the system Hilbert space. This equation preserves Hermiticity and trace of  $\hat{\rho}$ , as well as ensures non-negativity of all eigenvalues of  $\hat{\rho}$  at all times for all initial states of the system. The last condition crucially requires that  $\gamma_{\lambda} \geq 0$  [6,7]. This result is one of the cornerstones of open quantum systems. Indeed, a large number of analytical [8–10] and numerical [11–14] techniques rely on describing experimental systems via Lindblad equations.

The standard way to obtain a QME to leading order in system-bath coupling is via the Born-Markov approximation [8–10]. The QME so obtained, often called the Redfield equation (RE) [15], though reducible to a Lindblad-like form, is known to generically not satisfy complete positivity, i.e., not satisfy the requirement  $\gamma_{\lambda} \geq 0$  [16–22]. This means that for certain initial states and at certain times, it will not give a positive semidefinite density matrix. To rectify this drawback, typically, further approximations are made to obtain a Lindblad equation either in the so-called local or global forms, which we call local Lindblad equations (LLE) and eigenbasis Lindblad equations (ELE), respectively [8–10]. Several shortcomings of the LLE and ELE so obtained, in particular their failure to correctly describe the steady state when coupled to multiple baths, have been pointed out in the literature and their regimes of validity discussed [16,17,23–39]. Despite

\*djtupkary@uwaterloo.ca

†abhishek.dhar@icts.res.in

‡manas.kulkarni@icts.res.in

§archak.p@tcd.ie

this, the conventional wisdom is that, in principle, it should be possible to find a Lindblad equation, different from both LLE and ELE, which accurately describes the steady state. Indeed, there have been a number of recent attempts towards developing such new variants of Lindblad equations [40–45], which are intended to be as accurate as the RE.

Here, we lay down some fundamental requirements on any such attempt to recover complete positivity, which, if violated, causes physical inconsistencies such as inaccuracies in the leading order populations (diagonal elements of the density matrix) and coherences (off-diagonal elements of the density matrix) in the energy eigenbasis, violation of thermalization, and violation of local conservation laws in the nonequilibrium steady state (NESS). We show that the RE does not have any of the above physical inconsistencies, despite being generically not completely positive. On the other hand, we argue that no existing weak system-bath-coupling Lindblad description, to our knowledge, generically satisfies all the conditions, and therefore has one or more of the physical inconsistencies despite being completely positive. As an example, we study in detail the so-called universal Lindblad equation (ULE) [40], which has been recently rigorously derived to have accuracy comparable to that of the RE. We show that the ULE gives inaccurate coherences in the energy eigenbasis to the leading order and violates local conservation laws. All of the above statements are shown in complete generality for time-independent Hamiltonians, without writing any specific system Hamiltonian. This model-independent discussion sets apart our work from most previous works on checking the accuracy of various QMEs, where the accuracies were studied numerically in specific models [16,17,23–37]. We finally exemplify our discussion numerically in a three-site XXZ model coupled to two bosonic baths.

The paper is organized as follows. In Sec. II, we discuss the fundamental requirements. In Sec. III, we discuss how the RE satisfies all the fundamental requirements except complete positivity. In Sec. IV, we show that the ULE violates some of the fundamental requirements while restoring complete positivity and make some general comments about other Lindblad equations. In Sec. V, we numerically exemplify our discussions using the XXZ model. In Sec. VI, we summarize and conclude.

## II. FUNDAMENTAL REQUIREMENTS FOR AN ACCURATE WEAK-COUPLING MARKOVIAN DESCRIPTION

### A. The setup and assumptions

For simplicity and concreteness, let us consider a typical two-terminal setup of the form given in Fig. 1. The Hamiltonian of the full setup can be written in the form

$$\begin{aligned}\hat{H} &= \hat{H}_S + \epsilon \hat{H}_{SB} + \hat{H}_B, \\ \hat{H}_{SB} &= \hat{H}_{SB_L} + \hat{H}_{SB_R}, \quad \hat{H}_B = \hat{H}_{B_L} + \hat{H}_{B_R},\end{aligned}\quad (2)$$

where  $\hat{H}_S$  is the Hamiltonian of the system,  $\hat{H}_{B_L}$  ( $\hat{H}_{B_R}$ ) is the Hamiltonian of the left (right) bath,  $\hat{H}_{SB_L}$  ( $\hat{H}_{SB_R}$ ) is the coupling between the left (right) bath and the system, and the dimensionless parameter  $\epsilon$  controls the strength of the system-bath couplings. We consider the system-bath couplings to be

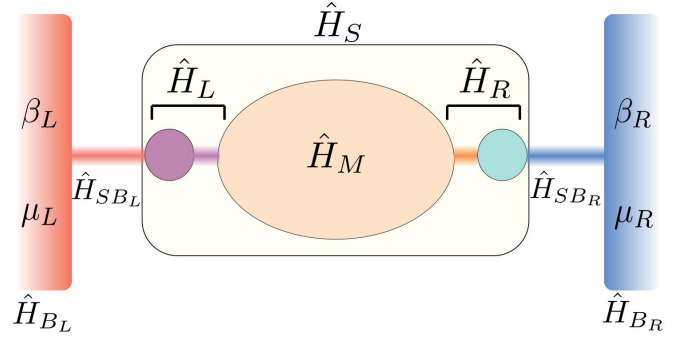


FIG. 1. A typical two-terminal nonequilibrium setup with not all sites attached to the baths. The Hamiltonian  $\hat{H}_M$  describes the part of  $\hat{H}_S$  that commutes with the system-bath-coupling Hamiltonians  $\hat{H}_{SB_L}$  and  $\hat{H}_{SB_R}$ , while the Hamiltonian  $\hat{H}_L$  ( $\hat{H}_R$ ) describes the part of the system Hamiltonian that does not commute with  $\hat{H}_{SB_L}$  ( $\hat{H}_{SB_R}$ ).

weak,  $\epsilon \ll 1$ . The system Hamiltonian is further broken into

$$\hat{H}_S = \hat{H}_L + \hat{H}_M + \hat{H}_R, \quad (3)$$

where  $\hat{H}_M$  contains the part of the system Hamiltonian that commutes with the system-bath-coupling Hamiltonians  $\hat{H}_{SB_L}$  and  $\hat{H}_{SB_R}$ , while,  $\hat{H}_L$  ( $\hat{H}_R$ ) contains the part of the system Hamiltonian that does not commute with  $\hat{H}_{SB_L}$  ( $\hat{H}_{SB_R}$ ). We will further assume for simplicity that the system Hamiltonian  $\hat{H}_S$  has no degeneracies. Initially, the system is at some arbitrary state, while the baths are at inverse temperatures  $\beta_L$  and  $\beta_R$ , and chemical potentials  $\mu_L$  and  $\mu_R$ . We take the total number of particles (excitations) in the whole setup to be conserved. Without loss of generality, it is possible to assume that  $\text{Tr}[\hat{H}_{SB}\hat{\rho}(0) \otimes \hat{\rho}_B] = 0$  [8], where  $\hat{\rho}_B$  denotes the composite state of the two baths given by the product of their individual thermal states. The state of the system at a time  $t$  is

$$\hat{\rho}(t) = \text{Tr}_B[e^{-i\hat{H}t} \hat{\rho}(0) \otimes \hat{\rho}_B e^{i\hat{H}t}], \quad (4)$$

where  $\text{Tr}_B(\cdot)$  implies trace over bath degrees of freedom. We will assume that in the long-time limit, the system reaches a unique NESS. This assumption physically necessitates that the system size is finite, while the baths are in the thermodynamic limit. The NESS density matrix is then defined as

$$\hat{\rho}_{\text{NESS}} = \lim_{t \rightarrow \infty} \text{Tr}_B[e^{-i\hat{H}t} \hat{\rho}(0) \otimes \hat{\rho}_B e^{i\hat{H}t}]. \quad (5)$$

With this concrete, but still fairly general setup and the assumptions in mind, we now look at what the fundamental requirements are for a weak-coupling QME to accurately describe the NESS of the system.

### B. The fundamental requirements

We want to have a Markovian QME, written to leading order in system-bath coupling, that accurately predicts the NESS density matrix. To this end, we require the following physical conditions:

(a) *Preservation of all properties of density matrix.* We want a QME of the form

$$\frac{\partial \hat{\rho}}{\partial t} = i[\hat{\rho}, \hat{H}_S] + \epsilon^2 \hat{\mathcal{L}}_2(\hat{\rho}), \quad (6)$$

where we have made it explicit that this equation is written to  $O(\epsilon^2)$ , which can be shown to be leading order [8]. To preserve all properties of the density matrix, i.e., (i) Hermiticity, (ii) trace, and (iii) complete positivity,  $\hat{\mathcal{L}}_2(\rho)$  must be reducible to the form of  $\hat{\mathcal{L}}(\rho)$  given in Eq. (1), with  $\gamma_\lambda \geq 0$ .

(b) *Correct populations and coherences in energy eigenbasis to the leading order.* Since we are making a weak-coupling approximation at the level of the QME, we cannot expect to have accurate results at NESS to all orders in  $\epsilon$ . But, we want to have results correct to at least the leading order. In particular, we want to have correct results for both populations and coherences in the energy eigenbasis at least to the leading order. Coherences in the energy eigenbasis of the system, as well as population inversions in the energy eigenbasis, have been considered to be a resource in quantum thermodynamics and information [46–56]. Thus, it is important to describe populations and coherences correctly. Moreover, as we will see later, both populations and coherences are crucially linked to having correct currents at NESS.

(c) *Thermalization.* Further, having correct populations to leading order is also linked with the fundamental phenomenon of thermalization of the system with the baths when they have same temperatures and chemical potentials,  $\beta_L = \beta_R = \beta$ ,  $\mu_L = \mu_R = \mu$ . In that case, on physical grounds, the steady-state density matrix is expected to satisfy the following condition:

$$\lim_{\epsilon \rightarrow 0} [\lim_{t \rightarrow \infty} \hat{\rho}(t)] = \frac{e^{-\beta(\hat{H}_S - \mu \hat{N}_S)}}{\text{Tr}(e^{-\beta(\hat{H}_S - \mu \hat{N}_S)}), \quad (7)$$

where  $\hat{N}_S$  is the total particle or excitation number operator of the system. In other words, populations of the density matrix in the energy eigenbasis of the system, to the leading order in system-bath coupling, should follow a Gibbs distribution specified by the temperature and the chemical potential of the baths when they are all equal. As we will show later, if the steady state is unique, this condition is always satisfied in the exact steady state [Eq. (5)]. Note that in Eq. (7), the order of limits cannot be interchanged.

(d) *Preservation of local conservation laws.* Writing the Heisenberg's equation of motion for our setup and taking trace, it is clear that the rate of change of the expectation value of any operator  $\hat{O}$  which commutes with the system-bath couplings is given by

$$\frac{d\langle \hat{O} \rangle}{dt} = -i\langle [\hat{O}, \hat{H}_S] \rangle, \quad \forall [\hat{O}, \hat{H}_{SB}] = 0, \quad (8)$$

where  $\langle \cdot \rangle = \text{Tr}(\hat{\rho} \dots)$ . This condition is obviously true irrespective of the strength of the system-bath couplings. We want our effective weak system-bath-coupling description to preserve this condition. Combining Eqs. (8) and (6), we see that this entails

$$\text{Tr}[\hat{O} \hat{\mathcal{L}}_2(\hat{\rho})] = 0, \quad \forall [\hat{O}, \hat{H}_{SB}] = 0. \quad (9)$$

This condition is not usually discussed in the context of deriving weak-coupling Markovian descriptions. However, the importance of this condition becomes clear when it is written for one of the locally conserved quantities, such as  $\hat{H}_M$ ,

$$\begin{aligned} \frac{d\langle \hat{H}_M \rangle}{dt} &= -i\langle [\hat{H}_M, \hat{H}_S] \rangle = J_{L \rightarrow M} - J_{M \rightarrow R}, \\ J_{L \rightarrow M} &= -i\langle [\hat{H}_M, \hat{H}_L] \rangle, \quad J_{M \rightarrow R} = i\langle [\hat{H}_M, \hat{H}_R] \rangle, \end{aligned} \quad (10)$$

where we have defined the energy current into the central region from the left as  $J_{L \rightarrow M}$ , and that from the central region to the right as  $J_{M \rightarrow R}$ . These currents are expectation values of some system operators and do not involve any explicit dependence on system-bath couplings. At NESS, the rate of change of the expectation values of all system operators is zero. Thus,  $\frac{d\langle \hat{H}_M \rangle}{dt} = 0$ , which implies  $J_{L \rightarrow M} = J_{M \rightarrow R}$ . So we have

$$\langle [\hat{H}_M, \hat{H}_L] \rangle = -\langle [\hat{H}_M, \hat{H}_R] \rangle \neq 0. \quad (11)$$

This is a fundamental property of the NESS that should exactly hold irrespective of the strength of the system-bath couplings. Equation (10), which at NESS leads to the above condition, is a continuity equation coming from the local conservation of energy. Analogous conditions can be derived for other locally conserved quantities. The QME written to leading order should satisfy all such conditions. It is clear that Eq. (9) guarantees this.

It can be seen that satisfying Eq. (9) and giving the correct rate of change of the expectation value of  $\hat{O}$  in Eq. (8) requires that the coherences in the energy eigenbasis are given correctly. To see this, we write the system Hamiltonian in the energy eigenbasis,

$$\hat{H}_S = \sum_{\alpha} E_{\alpha} |E_{\alpha}\rangle \langle E_{\alpha}|. \quad (12)$$

Using this basis, Eq. (8) can be written as

$$\begin{aligned} \frac{d\langle \hat{O} \rangle}{dt} &= -i \sum_{\alpha, v=1}^D (E_{\alpha} - E_v) \langle E_{\alpha} | \hat{\rho} | E_v \rangle \langle E_v | \hat{O} | E_{\alpha} \rangle, \\ \forall [\hat{O}, \hat{H}_{SB}] &= 0. \end{aligned} \quad (13)$$

Clearly, the right-hand side of above equation is governed by the coherences in the energy eigenbasis of the system. Thus, satisfying local conservation laws and obtaining correct currents at NESS requires the coherences to be correct (at least to leading order).

### C. The equations giving correct populations and coherences to the leading order

Let us now see what condition in terms of  $\hat{\mathcal{L}}_2$  must be satisfied so that the populations and the coherences in the energy eigenbasis are correct to the leading order. We assume that the NESS density matrix is defined in Eq. (5) and can be expanded in powers of  $\epsilon$ ,

$$\hat{\rho}_{\text{NESS}} = \sum_{m=0}^{\infty} \epsilon^{2m} \hat{\rho}_{\text{NESS}}^{(2m)}. \quad (14)$$

The QME describing the evolution of  $\hat{\rho}(t)$  can also be systematically expanded in the so-called time-convolution-less form [8],

$$\frac{\partial \hat{\rho}}{\partial t} = \sum_{m=0}^{\infty} \epsilon^{2m} \hat{\mathcal{L}}_{2m}(t) [\hat{\rho}(t)], \quad (15)$$

where  $\hat{\mathcal{L}}_{2m}(t)$  are, in general, time-dependent linear operators and  $\hat{\mathcal{L}}_0(t) [\hat{\rho}(t)] = i[\hat{\rho}(t), \hat{H}_S]$ . By definition, the steady state

$\hat{\rho}_{\text{NESS}}$  satisfies

$$0 = \sum_{m=0}^{\infty} \epsilon^{2m} \hat{\mathcal{L}}_{2m}[\hat{\rho}_{\text{NESS}}], \quad (16)$$

where we denote  $\hat{\mathcal{L}}_{2m} \equiv \hat{\mathcal{L}}_{2m}(t \rightarrow \infty)$ .

Using the series expansion of  $\hat{\rho}_{\text{NESS}}$  and matching terms order by order yields, at the lowest order ( $\epsilon^0$ ), the condition  $[\hat{\rho}_{\text{NESS}}^{(0)}, \hat{H}_S] = 0$ . This implies that  $\hat{\rho}_{\text{NESS}}^{(0)}$  is diagonal in the energy eigenbasis of the system,

$$\langle E_\alpha | \hat{\rho}_{\text{NESS}}^{(0)} | E_\nu \rangle = 0, \quad \forall \alpha \neq \nu. \quad (17)$$

This shows that while the populations can have the  $O(\epsilon^0)$  term, the leading order contribution to coherences in the energy eigenbasis is  $O(\epsilon^2)$ . (Remember that we have assumed no degeneracies in the system Hamiltonian.) This means  $\hat{\rho}_{\text{NESS}}^{(0)}$  can be written as

$$\hat{\rho}_{\text{NESS}}^{(0)} = \sum_{\alpha} p_{\alpha} |E_{\alpha}\rangle \langle E_{\alpha}|. \quad (18)$$

As a consequence, when the temperatures and the chemical potentials of the baths are equal,  $\beta_L = \beta_R = \beta$ ,  $\mu_L = \mu_R = \mu$ , the thermalization condition given by Eq. (7) requires

$$p_{\alpha} \propto e^{-\beta(E_{\alpha} - \mu N_{\alpha})}, \quad (19)$$

where  $N_{\alpha}$  is the number of particles or excitations in the energy eigenstate  $E_{\alpha}$ .

Let us now look at two higher orders in  $\epsilon$ . At order  $\epsilon^2$ , using Eq. (14) in Eq. (16) then leads to the following conditions:

$$\langle E_{\alpha} | \hat{\mathcal{L}}_2[\hat{\rho}_{\text{NESS}}^{(0)}] | E_{\alpha} \rangle = 0, \quad (20)$$

$$i(E_{\alpha} - E_{\nu}) \langle E_{\alpha} | \hat{\rho}_{\text{NESS}}^{(2)} | E_{\nu} \rangle + \langle E_{\alpha} | \hat{\mathcal{L}}_2[\hat{\rho}_{\text{NESS}}^{(0)}] | E_{\nu} \rangle = 0, \quad \forall \alpha \neq \nu, \quad (21)$$

and, at order  $\epsilon^4$ , we get

$$\langle E_{\alpha} | \hat{\mathcal{L}}_2[\hat{\rho}_{\text{NESS}}^{(2)}] | E_{\alpha} \rangle + \langle E_{\alpha} | \hat{\mathcal{L}}_4[\hat{\rho}_{\text{NESS}}^{(0)}] | E_{\alpha} \rangle = 0. \quad (22)$$

The set of equations obtained by writing Eq. (20) for various values of eigenstate index  $\alpha$  gives a complete set of equations which determines the nonzero elements of  $\hat{\rho}_{\text{NESS}}^{(0)}$ . Given  $\hat{\rho}_{\text{NESS}}^{(0)}$ , the set of equations obtained by writing Eq. (21) for various values of eigenstate indices  $\alpha$  and  $\nu$  determines the off-diagonal elements of  $\hat{\rho}_{\text{NESS}}^{(2)}$  in the energy eigenbasis. Finally, given the off-diagonal elements of  $\hat{\rho}_{\text{NESS}}^{(2)}$  in the energy eigenbasis, and the  $\hat{\rho}_{\text{NESS}}^{(0)}$ , the set of equations obtained by writing Eq. (22) for various values of the eigenstate index  $\alpha$  determines the diagonal elements of  $\hat{\rho}_{\text{NESS}}^{(2)}$ . It is crucial to note the occurrence of  $\hat{\mathcal{L}}_4$  in Eq. (22). Since the leading order populations are  $O(\epsilon^0)$  and the leading order coherences are  $O(\epsilon^2)$ , Eqs. (20) and (22) give the necessary equations to solve in order to obtain populations and coherences correct to the leading order. The above discussion corresponds to the NESS obtained from the exact QME, given by Eq. (15), in the regime of small  $\epsilon$ .

#### D. The need to go beyond standard Lindblad descriptions

In the previous section,  $\hat{\mathcal{L}}_2$  was derived from a time-convolution-less expansion. This fixes the form of  $\hat{\mathcal{L}}_2$ . If we

truncate the time-convolution-less expansion at  $O(\epsilon^2)$  and take the long-time limit, we get an equation that is exactly of our desired form in Eq. (6). This coincides with the Born-Markov approximation and gives the RE [8]. However, it is known that the RE does not generically satisfy the requirement of complete positivity [16–22]. Due to this, very often further approximations are made on  $\hat{\mathcal{L}}_2$ , modifying it to, say,  $\hat{\mathcal{L}}'_2$  so as to impose complete positivity. Our analysis in the previous sections allows us to impose some necessary restrictions on the approximations by fixing certain components of  $\hat{\mathcal{L}}'_2$ , so that the fundamental requirements are satisfied. The set of conditions is summarized in Table I. In particular, we see that for both populations and coherences to be correct to the leading order, we require the operation of  $\hat{\mathcal{L}}'_2$  on any state diagonal in the energy eigenbasis to be the same as that of  $\hat{\mathcal{L}}_2$ .

In most studies of the accuracy of the results from QMEs, the accuracy is checked by applying them to some particular system and comparing the results with some other more accurate method [16,17,23–38]. This does not let one clearly comment on situations where such more accurate methods are unavailable. The set of conditions in Table I allows us to assess the accuracy of  $\hat{\mathcal{L}}'_2$  by making formal checks, without explicitly writing it for any particular system. They therefore allow a completely general discussion of the accuracy of NESS results from QMEs, even in cases where some more accurate method is unavailable.

The most standard approximations on  $\hat{\mathcal{L}}_2$  involve reducing it to either the form of LLE or ELE. As mentioned before, it is already well established that the LLE and the ELE do not satisfy all the fundamental requirements mentioned in Sec. II B [16,17,23–38], and therefore do not satisfy all the conditions in Table I. The LLE does not show thermalization, while it explicitly satisfies the fourth condition in Table I, thereby preserving local conservation laws. On the other hand, the ELE explicitly neglects various coherences in the energy eigenbasis of the system, but satisfies thermalization [8]. Moreover, ELE does not also satisfy the fourth condition in Table I. Further, the ELE is known to not satisfy Eq. (11) because it gives zero currents inside the system, even in an out-of-equilibrium condition [24,28]. So neither of these standard Lindblad equations satisfy all the requirements above. This makes it necessary to go beyond these standard approximations, even at weak system-bath coupling.

In the following section, we consider the RE in more detail and show that even though the RE does not generically satisfy the requirement of complete positivity, it satisfies all of the other fundamental requirements.

### III. THE REDFIELD EQUATION

#### A. Accuracy of populations and coherences from the Redfield equation and lack of complete positivity

As mentioned before, the RE is obtained by truncating Eq. (15) at second order and replacing  $\hat{\mathcal{L}}_2(t)$  by  $\hat{\mathcal{L}}_2(t \rightarrow \infty) \equiv \hat{\mathcal{L}}_2$  [8],

$$\frac{\partial \hat{\rho}}{\partial t} = \hat{\mathcal{L}}_0[\hat{\rho}(t)] + \epsilon^2 \hat{\mathcal{L}}_2[\hat{\rho}(t)]. \quad (23)$$



TABLE I. Summary of necessary conditions that a QME written to the leading order in the system-bath coupling must satisfy to accurately describe the steady state of a setup of the form in Fig. 1.  $\hat{\mathcal{L}}_2$  is the  $O(\epsilon^2)$  term obtained by systematically doing time-convolution-less expansion and taking the long-time limit [see Eqs. (15) and (16)]. The  $\hat{\mathcal{L}}_2[\hat{\rho}]$  coincides with that obtained in the Redfield equation via the Born-Markov approximation and is known to generically not satisfy the complete positivity requirement  $\gamma_\lambda \geq 0$ . The  $\hat{\mathcal{L}}'_2$  is any modification of  $\hat{\mathcal{L}}_2$  which may restore complete positivity.

1. Correct populations to leading order [ $O(\epsilon^0)$ ]	$\langle E_\alpha   \hat{\mathcal{L}}'_2 [\sum_\alpha p_\alpha  E_\alpha\rangle\langle E_\alpha ]  E_\alpha\rangle = \langle E_\alpha   \hat{\mathcal{L}}_2 [\sum_\alpha p_\alpha  E_\alpha\rangle\langle E_\alpha ]  E_\alpha\rangle$
2. Correct coherences to leading order [ $O(\epsilon^2)$ ]	$\langle E_\alpha   \hat{\mathcal{L}}'_2 [\sum_\alpha p_\alpha  E_\alpha\rangle\langle E_\alpha ]  E_\nu\rangle = \langle E_\alpha   \hat{\mathcal{L}}_2 [\sum_\alpha p_\alpha  E_\alpha\rangle\langle E_\alpha ]  E_\nu\rangle, \forall \alpha \neq \nu$
3. Thermalization [Eq. (7)]	$\langle E_\alpha   \hat{\mathcal{L}}'_2 [\sum_\alpha p_\alpha  E_\alpha\rangle\langle E_\alpha ]  E_\alpha\rangle = 0 \Rightarrow p_\alpha \propto e^{-\beta(E_\alpha - \mu N_\alpha)}$ when $\beta_L = \beta_R = \beta, \mu_L = \mu_R = \mu$
4. Preservation of local conservation laws	$\text{Tr}[\hat{O} \hat{\mathcal{L}}'_2(\hat{\rho})] = 0, \forall [\hat{O}, \hat{H}_{SB}] = 0$
5. Complete positivity	$\hat{\mathcal{L}}'_2[\hat{\rho}] = i[\hat{\rho}, \hat{H}_{LS}] + \sum_{\lambda=1}^{D^2-1} \gamma_\lambda (\hat{L}_\lambda \hat{\rho} \hat{L}_\lambda^\dagger - \frac{1}{2} \{\hat{L}_\lambda^\dagger \hat{L}_\lambda, \hat{\rho}\}), \gamma_\lambda \geq 0$

The NESS obtained from the RE, which we denote by  $\tilde{\rho}_{\text{NESS}}$ , is given by

$$\tilde{\rho}_{\text{NESS}} = \lim_{t \rightarrow \infty} e^{t(\hat{\mathcal{L}}_0 + \hat{\mathcal{L}}_2)}[\rho(0)], \quad (24)$$

and satisfies

$$0 = \hat{\mathcal{L}}_0[\tilde{\rho}_{\text{NESS}}] + \epsilon^2 \hat{\mathcal{L}}_2[\tilde{\rho}_{\text{NESS}}]. \quad (25)$$

The density matrix can also be expanded in powers of  $\epsilon$ ,  $\tilde{\rho}_{\text{NESS}} = \sum_{m=0}^{\infty} \epsilon^{2m} \tilde{\rho}_{\text{NESS}}^{(2m)}$ . The question then is, to what order in  $\epsilon$  do the elements of  $\tilde{\rho}_{\text{NESS}}$  and  $\hat{\rho}_{\text{NESS}}$  agree?

Proceeding as before, we again get  $[\tilde{\rho}_{\text{NESS}}^{(0)}, \hat{H}_S] = 0$ , implying a diagonal  $\tilde{\rho}_{\text{NESS}}^{(0)}$  in the energy eigenbasis. At  $O(\epsilon^2)$ , we now obtain

$$\langle E_\alpha | \hat{\mathcal{L}}_2[\tilde{\rho}_{\text{NESS}}^{(0)}] |E_\alpha\rangle = 0, \quad (26)$$

$$i(E_\alpha - E_\nu) \langle E_\alpha | \tilde{\rho}_{\text{NESS}}^{(2)} |E_\nu\rangle + \langle E_\alpha | \hat{\mathcal{L}}_2[\tilde{\rho}_{\text{NESS}}^{(0)}] |E_\nu\rangle = 0, \quad \forall \alpha \neq \nu, \quad (27)$$

while at  $O(\epsilon^4)$ , we get

$$\langle E_\alpha | \hat{\mathcal{L}}_2[\tilde{\rho}_{\text{NESS}}^{(2)}] |E_\alpha\rangle = 0. \quad (28)$$

Equations (26), (27), and (28) are the analogs of Eqs. (20), (21), and (22), respectively. We see from Eqs. (20) and (26) that  $\tilde{\rho}_{\text{NESS}}^{(0)}$  and  $\hat{\rho}_{\text{NESS}}^{(0)}$  satisfy the exact same set of equations, which implies

$$\tilde{\rho}_{\text{NESS}}^{(0)} = \hat{\rho}_{\text{NESS}}^{(0)}. \quad (29)$$

Next, from Eqs. (21) and (27), we see that the off-diagonal elements of  $\tilde{\rho}_{\text{NESS}}^{(2)}$  and  $\hat{\rho}_{\text{NESS}}^{(2)}$  in the energy eigenbasis also satisfy exactly the same equation, therefore implying

$$\langle E_\alpha | \tilde{\rho}_{\text{NESS}}^{(2)} |E_\nu\rangle = \langle E_\alpha | \hat{\rho}_{\text{NESS}}^{(2)} |E_\nu\rangle, \quad \forall \alpha \neq \nu. \quad (30)$$

Thus, the leading order terms in the populations and coherences are given correctly by the RE. However, Eq. (22), which fixes the diagonal elements of  $\hat{\rho}_{\text{NESS}}^{(2)}$  in the energy eigenbasis, is different from Eq. (28), which fixes the same for  $\tilde{\rho}_{\text{NESS}}^{(2)}$ . So,

$$\langle E_\alpha | \tilde{\rho}_{\text{NESS}}^{(2)} |E_\alpha\rangle \neq \langle E_\alpha | \hat{\rho}_{\text{NESS}}^{(2)} |E_\alpha\rangle. \quad (31)$$

Specifically, Eq. (22) shows that to obtain the diagonal elements of the NESS density matrix in the energy eigenbasis

correct to  $O(\epsilon^2)$ , one needs the QME up of  $O(\epsilon^4)$ . Based on these results, we have

$$\|\hat{\rho}_{\text{NESS}} - \tilde{\rho}_{\text{NESS}}\| \sim O(\epsilon^2), \quad (32)$$

where  $\|\hat{P}\|$  is the norm of the operator  $\hat{P}$ . So, the error in obtaining the NESS from Eq. (23) is  $O(\epsilon^2)$ . Despite this, the leading order coherences in the energy eigenbasis, which are  $O(\epsilon^2)$ , are given correctly. Having the  $O(\epsilon^2)$  term in the coherences accurately while not having the corresponding correction in the populations can cause, at  $O(\epsilon^2)$ , a violation of positivity of the density matrix [57,58]. Thus, the lack of complete positivity of the RE stems from the above mismatch in order of accuracy between populations and coherences.

## B. Thermalization

The explicit form of Eq. (23) is given by (Eq. (9.52) of Ref. [8])

$$\frac{\partial \hat{\rho}}{\partial t} = i[\hat{\rho}(t), H_S] + \epsilon^2 \int_0^\infty dt' [\hat{H}_{SB}, [\hat{H}_{SB}(-t'), \hat{\rho}(t) \otimes \hat{\rho}_B]], \quad (33)$$

where  $\hat{H}_{SB}(t) = e^{i(\hat{H}_S + \hat{H}_B)t} \hat{H}_{SB} e^{-i(\hat{H}_S + \hat{H}_B)t}$ . Let us now consider the following canonical model of thermal baths:

$$\hat{H}_B = \sum_{\ell} \sum_{r=1}^{\infty} \Omega_r^\ell \hat{B}_r^{(\ell)\dagger} \hat{B}_r^{(\ell)}, \quad (34)$$

$$\hat{H}_{SB} = \sum_{\ell} \sum_{r=1}^{\infty} (\kappa_{\ell r} \hat{B}_r^{(\ell)\dagger} \hat{S}_\ell + \kappa_{\ell r}^* \hat{S}_\ell \hat{B}_r^{(\ell)}), \quad (35)$$

where  $\sum_{\ell}$  indicates the sum over all sites of the system where the baths are attached,  $\hat{B}_r^{(\ell)}$  is the bosonic or fermionic annihilation operator for the  $r$ th mode of the bath attached at the  $\ell$ th site, and  $\hat{S}_\ell$  is the system operator coupling to the bath at site  $\ell$ . At the initial time, the baths are taken to be in their respective thermal state with inverse temperatures  $\beta_\ell$  and chemical potentials  $\mu_\ell$ . The dynamics of the system can be shown to be governed by the bath spectral functions, defined as

$$\mathfrak{J}_\ell(\omega) = \sum_k 2\pi |\kappa_{\ell k}|^2 \delta(\omega - \Omega_k^\ell), \quad (36)$$

and the Fermi or Bose distributions,  $n_\ell(\omega) = [e^{\beta_\ell(\omega - \mu_\ell)} \pm 1]^{-1}$ , corresponding to the initial states of the baths. The RE

for this setup is obtained by simplification of Eq. (33), using Eqs. (34) and (35):

$$\frac{\partial \hat{\rho}}{\partial t} = i[\hat{\rho}, \hat{H}_S] - \epsilon^2 \sum_{\ell} ([\hat{S}_{\ell}^{\dagger}, \hat{S}_{\ell}^{(1)} \hat{\rho}] + [\hat{\rho} \hat{S}_{\ell}^{(2)}, \hat{S}_{\ell}^{\dagger}] + \text{H.c.}), \quad (37)$$

where

$$\begin{aligned} \hat{S}_{\ell}^{(1)} &= \int_0^{\infty} dt' \int \frac{d\omega}{2\pi} \hat{S}_{\ell}(-t') e^{\beta_{\ell}(\omega - \mu_{\ell})} \mathfrak{J}_{\ell}(\omega) n_{\ell}(\omega) e^{-i\omega t'}, \\ \hat{S}_{\ell}^{(2)} &= \int_0^{\infty} dt' \int \frac{d\omega}{2\pi} \hat{S}_{\ell}(-t') \mathfrak{J}_{\ell}(\omega) n_{\ell}(\omega) e^{-i\omega t'}, \end{aligned} \quad (38)$$

with  $\hat{S}_{\ell}(t) = e^{i\hat{H}_S t} \hat{S}_{\ell} e^{-i\hat{H}_S t}$ , and H.c. denoting Hermitian conjugate. Note that, in general,  $[\hat{S}_{\ell}, \hat{S}_{\ell}^{(1)}] \neq 0$ ,  $[\hat{S}_{\ell}, \hat{S}_{\ell}^{(2)}] \neq 0$ . Let us now check if the RE satisfies the thermalization condition given in Eq. (7). To this end, we need to find the leading order populations when the temperatures and chemical potentials of the baths are the same,  $\beta_L = \beta_R = \beta$ ,  $\mu_L = \mu_R = \mu$ . Defining  $E_{v\alpha} = E_v - E_{\alpha}$  and writing  $\hat{\rho}_{\text{NESS}}^{(0)} = \sum_{\alpha} p_{\alpha} |E_{\alpha}\rangle \langle E_{\alpha}|$ , it can be checked after some algebra that Eq. (26), for the RE in Eq. (37), takes the form

$$\begin{aligned} &\sum_{\nu} [|\langle E_{\nu} | \hat{S}_{\ell} | E_{\alpha} \rangle|^2 [p_{\alpha} - e^{\beta(E_{\nu\alpha} - \mu)} p_{\nu}] \mathfrak{J}_{\ell}(E_{\nu\alpha}) n_{\ell}(E_{\nu\alpha}) \\ &\quad + |\langle E_{\alpha} | \hat{S}_{\ell} | E_{\nu} \rangle|^2 [p_{\nu} - e^{\beta(E_{\alpha\nu} - \mu)} p_{\alpha}] \mathfrak{J}_{\ell}(E_{\alpha\nu}) n_{\ell}(E_{\alpha\nu})] \\ &= 0. \end{aligned} \quad (39)$$

We now consider the case where the system operator coupling to the bath can create or annihilate a single particle, i.e.,  $\langle E_{\nu} | \hat{S}_{\ell} | E_{\alpha} \rangle = 0$ ,  $\forall N_{\alpha} - N_{\nu} \neq 1$ . This condition ensures that with the system-bath coupling of the form in Eq. (35), the total number of excitations in the full setup is conserved. It can then be checked that the following choice of  $p_{\alpha}$  satisfies the above equation:

$$p_{\alpha} \propto e^{-\beta(E_{\alpha} - \mu N_{\alpha})}. \quad (40)$$

Since we have assumed the steady state to be unique, this proves that the thermalization condition, i.e., the third condition in Table I, is satisfied.

Note that since the leading order populations obtained from RE are exactly the same as those obtained from the full general time-convolution-less Eq. (15), the above proof of thermalization is essentially a proof of thermalization for the full time-convolution-less Eq. (15). Thus, if the steady state is unique, the thermalization condition is satisfied in complete generality. So, any Lindblad equation that does not satisfy this condition (such as the LLE) cannot describe the steady state of a system coupled to thermal baths.

### C. Satisfying local conservation laws

Given the RE [Eq. (37)], one can write an expression for expectation value of any system operator  $O$ ,

$$\begin{aligned} \frac{d \langle \hat{O} \rangle}{dt} &= -i \langle [\hat{O}, \hat{H}_S] \rangle - \epsilon^2 \sum_{\ell} ([\langle \hat{O}, \hat{S}_{\ell}^{\dagger} \rangle \hat{S}_{\ell}^{(1)}] - \langle \hat{S}_{\ell}^{(2)} [\hat{O}, \hat{S}_{\ell}^{\dagger}] \rangle \\ &\quad + \langle \hat{S}_{\ell}^{(1)\dagger} [\hat{S}_{\ell}, \hat{O}] \rangle - \langle [\hat{S}_{\ell}, \hat{O}] \hat{S}_{\ell}^{(2)\dagger} \rangle). \end{aligned} \quad (41)$$

It is clear from the above expression that the fourth condition in Table I is satisfied. Thus, it is clear that the local conservation laws inside the system are satisfied. Not only that, as we show below, further conservation laws relating currents from the baths and currents inside the system are also satisfied.

For the kind of setup in Fig. 1, the RE can be written as

$$\frac{\partial \hat{\rho}}{\partial t} = i[\hat{\rho}, \hat{H}_S] + \epsilon^2 (\hat{\mathcal{L}}_2^{(L)}[\hat{\rho}(t)] + \hat{\mathcal{L}}_2^{(R)}[\hat{\rho}(t)]), \quad (42)$$

where  $\hat{\mathcal{L}}_2^{(L)}[\hat{\rho}(t)]$  ( $\hat{\mathcal{L}}_2^{(R)}[\hat{\rho}(t)]$ ) encodes the effect of the left (right) bath, with the full superoperator being  $\hat{\mathcal{L}}_2[\hat{\rho}(t)] = \hat{\mathcal{L}}_2^{(L)}[\hat{\rho}(t)] + \hat{\mathcal{L}}_2^{(R)}[\hat{\rho}(t)]$ . Using this, we can write the equation for the rate of change of energy in the system,

$$\frac{d \langle \hat{H}_S \rangle}{dt} = J_{B_L} + J_{B_R}, \quad J_{B_L} = \epsilon^2 \text{Tr}(\hat{H}_S \hat{\mathcal{L}}_2^{(L)}[\rho(t)]), \quad (43)$$

$$J_{B_R} = \epsilon^2 \text{Tr}(\hat{H}_S \hat{\mathcal{L}}_2^{(R)}[\rho(t)]), \quad (44)$$

where  $J_{B_L}$  ( $J_{B_R}$ ) can be interpreted as the energy current from the left (right) bath into the system.

Next, let us look at the relation between the currents from the baths and the currents in the system. Due to local conservation of energy, the following continuity equations must be satisfied:

$$\frac{d \langle \hat{H}_L \rangle}{dt} = J_{B_L} - J_{L \rightarrow M}, \quad \frac{d \langle \hat{H}_R \rangle}{dt} = J_{B_R} + J_{M \rightarrow R}, \quad (45)$$

where  $J_{L \rightarrow M}$  and  $J_{M \rightarrow R}$  are defined in Eq. (10). Satisfying this condition requires that along with Eq. (9), the following relation is satisfied:

$$\begin{aligned} \text{Tr}(\hat{H}_{\ell} \hat{\mathcal{L}}_2^{(L)}[\rho(t)]) + \text{Tr}(\hat{H}_{\ell} \hat{\mathcal{L}}_2^{(R)}[\rho(t)]) &= \text{Tr}(\hat{H}_S \hat{\mathcal{L}}_2^{(\ell)}[\rho(t)]), \\ \ell &= L, R. \end{aligned} \quad (46)$$

From Eqs. (42) and (44), we can show that this condition is indeed satisfied and the local continuity equation relating the currents from the bath and the currents inside the system holds. At NESS, since the rate of change of all the system operators goes to zero, we have

$$J_{B_L} = J_{L \rightarrow M} = J_{M \rightarrow R} = -J_{B_R}. \quad (47)$$

This, once again, is a fundamental property of NESS, which is preserved by the RE.

The above discussion is with energy currents, but it holds true for any other currents associated with other local conserved quantities, for example, particle currents.

### D. Accuracy of currents from RE

Although the local continuity equations are always satisfied by RE, the currents obtained from RE are only accurate to  $O(\epsilon^2)$ . This can be seen noting that the currents inside the system are given by coherences in the energy eigenbasis, as shown by Eqs. (10) and (13). To see this explicitly, we write  $J_{L \rightarrow M}$  in the steady state as

$$\begin{aligned} J_{L \rightarrow M} &= -i \langle [\hat{H}_M, \hat{H}_L] \rangle \\ &= -i \langle [\hat{H}_S, \hat{H}_L] \rangle \\ &= i \sum_{\alpha, \nu=1}^D (E_{\alpha} - E_{\nu}) \langle E_{\alpha} | \hat{\rho}_{\text{NESS}} | E_{\nu} \rangle \langle E_{\nu} | \hat{H}_L | E_{\alpha} \rangle \end{aligned}$$

$$\begin{aligned}
 &= i\epsilon^2 \sum_{\alpha, \nu=1}^D (E_\alpha - E_\nu) \langle E_\alpha | \hat{\rho}_{\text{NESS}}^{(2)} | E_\nu \rangle \langle E_\nu | \hat{H}_L | E_\alpha \rangle \\
 &+ \text{higher orders.} \quad (48)
 \end{aligned}$$

In the last line, we have used the fact that the leading order coherences are  $O(\epsilon^2)$ . Since the coherences obtained from RE are given correctly only to  $O(\epsilon^2)$ , any higher-order term obtained from the RE cannot be trusted. Similar expressions can be written for  $J_{M \rightarrow R}$  or any other currents related to other local conserved quantities.

The fact that currents obtained from RE are correct to  $O(\epsilon^2)$  can also be seen by calculating the currents from the baths. Carrying out the trace in Eq. (44) in the energy eigenbasis of the system, the currents from the baths can be written as

$$\begin{aligned}
 J_{B_\ell} &= \epsilon^2 \sum_{\alpha} E_\alpha \langle E_\alpha | \mathcal{L}_2^{(\ell)} [\hat{\rho}_{\text{NESS}}^{(0)}] | E_\alpha \rangle \\
 &+ \epsilon^4 \sum_{\alpha} E_\alpha \langle E_\alpha | \hat{\mathcal{L}}_2^{(\ell)} [\hat{\rho}_{\text{NESS}}^{(2)}] | E_\alpha \rangle \\
 &+ \text{higher orders, where } \ell = L, R. \quad (49)
 \end{aligned}$$

This shows that the leading order currents from the baths are  $O(\epsilon^2)$  and depend on  $\hat{\rho}_{\text{NESS}}^{(0)}$  which, as shown before, is diagonal in the energy eigenbasis and is given correctly by the RE. In other words, the leading order currents from the baths are determined by the leading order populations in the energy eigenbasis. On the other hand, the  $O(\epsilon^4)$  term contains contributions from both the diagonal and the off-diagonal elements of  $\hat{\rho}_{\text{NESS}}^{(2)}$  in the energy eigenbasis of the system. Since the diagonal elements of  $\hat{\rho}_{\text{NESS}}^{(2)}$  in the energy eigenbasis of the system are not given correctly by RE, currents from RE will carry  $O(\epsilon^4)$  error.

A particularly critical condition arises when, on physical grounds, the currents are zero, for example, when the temperatures and the chemical potentials of the baths are the same,  $\beta_L = \beta_R = \beta$ ,  $\mu_L = \mu_R = \mu$ . In this case, the  $O(\epsilon^2)$  contribution to currents obtained from RE will be zero since this is given correctly. But, the  $O(\epsilon^4)$  term, which can contain an error, may not be zero. This will give unphysical  $O(\epsilon^4)$  currents even when the current is expected to be zero on physical grounds. Knowing this, it is, however, possible to clearly identify such spurious unphysical currents stemming from inaccuracies of RE by checking the scaling of the currents with  $\epsilon$ . If the scaling is  $O(\epsilon^2)$ , the currents obtained from RE can be trusted. If the scaling is  $O(\epsilon^4)$ , it shows that the  $O(\epsilon^2)$  contribution to the currents is zero. The currents must be taken as zero within the accuracy of RE in that case. This was explicitly used in Ref. [58] (see the supplemental material of Ref. [58]).

Another interesting point to note from Eqs. (48), (49), and (47) is that the  $O(\epsilon^2)$  coherences, the  $O(\epsilon^0)$  populations in the energy eigenbasis, and the preservation of local conservation laws are tightly related to one another. If either one of the populations and the coherences is given accurately, while the other is not, it will lead to violation of the local continuity equations.

It is clear from the discussion in this section that the only drawback of the RE is the lack of complete positivity. In the next section, we look in detail at one recent attempt to rigorously rectify this drawback, and show that it violates some of the other required conditions in Table I. We also make some general comments on all existing weak system-bath-coupling Lindblad descriptions.

#### IV. THE UNIVERSAL LINDBLAD EQUATION

As mentioned before, we need to go beyond the standard Lindblad equations in local and eigenbasis forms, LLE and ELE, to satisfy the required conditions in Table I. Since the RE is microscopically derived and satisfies all other requirements except for the complete positivity, it is intuitive that any QME satisfying the required conditions should give results close to RE. Recently, a Lindblad equation, called the universal Lindblad equation (ULE) [40], was rigorously derived such that it is of Lindblad form, while maintaining

$$\|\hat{\rho}_{\text{NESS}}^{\text{ULE}} - \hat{\rho}_{\text{NESS}}\| \sim \|\hat{\rho}_{\text{NESS}} - \hat{\rho}_{\text{NESS}}\| \sim O(\epsilon^2), \quad (50)$$

where  $\hat{\rho}_{\text{NESS}}^{\text{ULE}}$  is the NESS density matrix obtained from ULE. The ULE reduces to the LLE and the ELE with further approximations in appropriate limits [40]. Moreover, as discussed in [40,42], it is closely related to other recently derived Lindblad equations to go beyond ELE and LLE. This makes the study of ULE in light of the fundamental requirements representative of existing Lindblad equation approaches.

##### A. The general form of ULE

The ULE approach requires the system-bath coupling to be written in terms of Hermitian operators. So we write the system-bath coupling as  $\hat{H}_{SB} = \sum_{\ell} \sum_{k=1,2} \hat{X}_{(\ell,k)} \hat{B}_{(\ell,k)}$ , where

$$\begin{aligned}
 \hat{X}_{(\ell,1)} &= \hat{S}_{\ell}^{\dagger} + \hat{S}_{\ell}, \quad \hat{X}_{(\ell,2)} = i(\hat{S}_{\ell} - \hat{S}_{\ell}^{\dagger}), \\
 \hat{B}_{(\ell,1)} &= \sum_{r=1}^{\infty} \frac{\kappa_{r\ell} \hat{B}_r^{(\ell)\dagger} + \kappa_{r\ell}^* \hat{B}_r^{(\ell)}}{2}, \\
 \hat{B}_{(\ell,2)} &= i \sum_{r=1}^{\infty} \frac{\kappa_{r\ell}^* \hat{B}_r^{(\ell)} - \kappa_{r\ell} \hat{B}_r^{(\ell)\dagger}}{2}. \quad (51)
 \end{aligned}$$

The system-bath coupling is then given in the form

$$\hat{H}_{SB} = \sum_{\lambda} \hat{X}_{\lambda} \hat{B}_{\lambda}, \quad (52)$$

where  $\lambda = (\ell, k)$  is the combined index. The ULE is of the form

$$\begin{aligned}
 \frac{\partial \hat{\rho}}{\partial t} &= i[\hat{\rho}, \hat{H}_S] + \epsilon^2 \hat{\mathcal{L}}_2'[\hat{\rho}], \\
 \hat{\mathcal{L}}_2'[\hat{\rho}] &= i[\hat{\rho}, \hat{H}_{LS}] + \sum_{\lambda} \left( \hat{L}_{\lambda} \hat{\rho} \hat{L}_{\lambda}^{\dagger} - \frac{1}{2} \{ \hat{L}_{\lambda}^{\dagger} \hat{L}_{\lambda}, \hat{\rho} \} \right), \quad (53)
 \end{aligned}$$

with the Lindblad operators and the Lamb-shift Hamiltonian given by

$$\begin{aligned}
 \hat{L}_{\lambda} &= \sum_{\lambda'} \int_{-\infty}^{\infty} ds \tilde{\mathbf{g}}_{\lambda, \lambda'}(s) \hat{X}_{\lambda'}(-s), \\
 \hat{H}_{LS} &= \frac{1}{2i} \int_{-\infty}^{\infty} ds \int_{-\infty}^{\infty} ds' \sum_{\lambda, \lambda'} \hat{X}_{\lambda}(s) \hat{X}_{\lambda'}(s') \phi_{\lambda, \lambda'}(s, s'), \quad (54)
 \end{aligned}$$

where  $\hat{X}_\lambda(t) = e^{i\hat{H}_S t} \hat{X}_\lambda e^{-i\hat{H}_S t}$  denotes the interaction picture operator. The matrices  $\phi(t, s)$  and  $\tilde{g}(t)$  are

$$\begin{aligned} \tilde{g}(t) &= \int_{-\infty}^{\infty} d\omega g(\omega) e^{-i\omega t}, \quad \phi(t, s) = \tilde{g}(t) \tilde{g}(-s) \text{sgn}(t-s), \\ g(\omega) &= \sqrt{\frac{G(\omega)}{2\pi}}, \quad G_{\lambda, \lambda'}(\omega) = \int_{-\infty}^{\infty} \frac{dt}{2\pi} \langle \hat{B}_\lambda(t) \hat{B}_{\lambda'}(0) \rangle_B e^{i\omega t}, \end{aligned} \quad (55)$$

with  $\text{sgn}(x)$  being the sign function, and  $\langle \cdot \rangle_B$  denoting the expectation value taken over the bath initial state. Given this general form of the ULE, we now investigate if the ULE satisfies the fundamental requirements in Table I.

## B. Accuracy of ULE

### 1. Accurate populations but inaccurate coherences

As mentioned before, the ULE has been derived so that the steady state it predicts differs from the exact steady state in  $O(\epsilon^2)$ . This means that the  $O(\epsilon^0)$  term of the NESS density matrix must be given correctly by the ULE, and hence would match that from RE. Here we explain how to see this explicitly, in general.

For this, we write  $\hat{\rho}_{\text{NESS}}^{(0)}$  in the energy eigenbasis, as in Eq. (18), and explicitly evaluate the term required by the first condition in Table I,

$$\begin{aligned} &\langle E_\alpha | \hat{\mathcal{L}}_2' [\hat{\rho}_{\text{NESS}}^{(0)}] | E_\alpha \rangle \\ &= \sum_{\nu, \lambda, \lambda'} 2\pi p_\nu \left\{ \langle E_\alpha | \hat{X}_{\lambda'} | E_\nu \rangle \langle E_\nu | \hat{X}_\lambda | E_\alpha \rangle G_{\lambda, \lambda'}(E_\nu - E_\alpha) \right. \\ &\quad \left. - \sum_\gamma \langle E_\alpha | \hat{X}_\lambda | E_\gamma \rangle \langle E_\gamma | \hat{X}_{\lambda'} | E_\alpha \rangle G_{\lambda, \lambda'}(E_\alpha - E_\gamma) \delta_{\alpha\nu} \right\}. \end{aligned} \quad (56)$$

We need to compare this result with that obtained from RE to check the first condition in Table I. To do this, it is easier to write the RE also in the form where the system-bath-coupling terms are Hermitian operators, as in Eq. (52). The RE for this form of coupling is given by

$$\frac{\partial \hat{\rho}}{\partial t} = i[\hat{\rho}, \hat{H}_S] - \epsilon^2 \sum_{\lambda, \lambda'} ([\hat{X}_\lambda, \hat{X}_{\lambda'} \hat{\rho}] + \text{H.c.}), \quad (57)$$

with

$$\begin{aligned} \hat{X}_{\lambda'\lambda} &= \int_0^\infty dt' \langle \hat{B}_\lambda(t') \hat{B}_{\lambda'}(0) \rangle \hat{X}_{\lambda'}(-t') \\ &= \int_0^\infty dt' \int_{-\infty}^\infty G_{\lambda, \lambda'}(\omega) e^{-i\omega t'} \hat{X}_{\lambda'}(-t'). \end{aligned} \quad (58)$$

Using Eq. (51), it can be checked that Eq. (57) can be reduced to Eq. (37). With Eq. (57), direct evaluation of  $\langle E_\alpha | \hat{\mathcal{L}}_2' [\hat{\rho}_{\text{NESS}}^{(0)}] | E_\alpha \rangle$  gives exactly the same expression as Eq. (56). Thus the ULE explicitly satisfies the first condition in Table I. Therefore, the leading order populations obtained from ULE are the same as those from RE. It follows that ULE also satisfies the thermalization condition, i.e., the third condition in Table I. It is important to note that we do not

explicitly require the values of the populations  $p_\nu$  to show that the conditions are satisfied.

Using exactly similar steps, it can be checked that the ULE does not satisfy the second condition in Table I. Thus, the leading order coherences from ULE are not given correctly. Since the leading order coherences in the energy eigenbasis are  $O(\epsilon^2)$ , this is consistent with the ULE having an error of  $O(\epsilon^2)$  [see Eq. (50)].

### 2. Violation of local conservation laws

As we have already discussed, having correct populations to leading order while having incorrect coherences leads to the violation of local conservation laws. So, the ULE does not satisfy the fourth requirement in Table I. This can be explicitly seen by writing the evolution equation for any system operator,

$$\begin{aligned} \frac{d \langle \hat{O} \rangle}{dt} &= -i \langle [\hat{O}, \hat{H}_S + \hat{H}_{\text{LS}}] \rangle \\ &\quad + \sum_\lambda \frac{1}{2} (\langle [\hat{L}_\lambda^\dagger, \hat{O}] \hat{L}_\lambda \rangle + \langle \hat{L}_\lambda^\dagger [\hat{O}, \hat{L}_\lambda] \rangle). \end{aligned} \quad (59)$$

From the form of the operators  $\hat{L}_\lambda$  in Eq. (54), we see that even if  $[\hat{O}, \hat{H}_{SB}] = 0$ ,  $\text{Tr}[\hat{O} \hat{\mathcal{L}}_2'(\hat{\rho})] \neq 0$ .

### 3. Accuracy of currents from ULE

Despite this violation of local conservation laws, the ULE gives the correct currents from the baths to the leading order. This can be seen by writing the ULE in the form of Eq. (42) and defining the corresponding currents as in Eq. (44). The currents can then be written in the energy eigenbasis, as in Eq. (49), to see that the leading order contributions are given by the  $O(\epsilon^0)$  populations in the energy eigenbasis. Since these terms are given accurately by the ULE, it follows that the currents from the baths are given accurately to  $O(\epsilon^2)$  and agree with the same currents obtained from RE. The error in the currents from the baths as obtained from ULE is therefore  $O(\epsilon^4)$ , which is the same as that from RE.

However, since the coherences in the energy eigenbasis contain  $O(\epsilon^2)$  error in ULE, the currents inside the system, defined in Eq. (10), will have an error in the leading order. This, once again, shows that local conservation laws will be violated. Note that this is true even when the temperatures and chemical potentials of all the baths are the same. So, even though the ULE satisfies the thermalization condition (the third condition in Table I), due to incorrect coherences, it can give unphysical  $O(\epsilon^2)$  currents inside the system in the absence of any temperature or chemical potential bias.

### C. General comments regarding Lindblad equations

We end this section with some general comments regarding Lindblad equations. We have already mentioned that the ULE is closely related to some of the other Lindblad equations devised to go beyond the limitations of ELE and LLE. It is worth mentioning that to our knowledge, all existing Lindblad equations [40–45] except the LLE violate the fourth condition in Table I, thereby violating local conservation laws. The LLE, on the other hand, is known to not satisfy the thermalization requirement, the third condition in Table I. Further,



although explicitly satisfying the local conservation laws, it does not always give the correct currents in NESS [16,17,23–38]. This is contrary to the ULE, which, despite violating local conservation laws, gives correct currents from the baths to the leading order. The RE, on the other hand, except for generically violating the requirement of complete positivity, satisfies all other the conditions in Table I. It therefore seems that a weak system-bath-coupling QME respecting all the conditions in Table I is generically impossible. In particular, since currents inside the system are related to coherences, and currents from the baths are related to populations, it seems that no weak system-bath-coupling QME can generically satisfy the requirement of complete positivity and simultaneously give correct populations and coherences to the leading order. Thus, all weak system-bath-coupling Lindblad equations seem fundamentally limited. While this is true for the existing QMEs to our knowledge, a general proof of the fact is still missing. We leave the general proof of this to future work. Although all the results above have been derived keeping a setup of the form of Fig. 1 in mind, these can be easily carried forward to cases where there are more than two baths.

Our discussion until now has been general. We have not yet written any particular system Hamiltonian or chosen any particular bath spectral function. This completely general discussion of the accuracy of QMEs sets apart our work from most previous works [16,17,23–38], where the accuracy is discussed referring to a particular model. In the following, we numerically check our general discussion in the three-site Heisenberg model coupled to bosonic baths.

## V. NUMERICAL RESULTS

We now numerically exemplify the above discussion by using a XXZ spin chain in the presence of a magnetic field, with the first and the last sites attached to baths modeled by infinite number of bosonic modes,

$$\begin{aligned} \hat{H}_S &= \sum_{\ell=1}^N \frac{\omega_0^{(\ell)}}{2} \hat{\sigma}_z^\ell - \sum_{\ell=1}^{N-1} g (\hat{\sigma}_x^\ell \hat{\sigma}_x^{\ell+1} + \hat{\sigma}_y^\ell \hat{\sigma}_y^{\ell+1} + \Delta \hat{\sigma}_z^\ell \hat{\sigma}_z^{\ell+1}), \\ \hat{H}_{SB} &= \sum_{\ell=1, N} \sum_{r=1}^{\infty} (\kappa_{\ell r} \hat{B}_r^{(\ell)\dagger} \hat{\sigma}_-^\ell + \kappa_{\ell r}^* \hat{B}_r^{(\ell)} \hat{\sigma}_+^\ell), \end{aligned} \quad (60)$$

where  $\hat{\sigma}_{x,y,z}^\ell$  denotes the Pauli matrices acting on the  $\ell$ th spin,  $\hat{\sigma}_+^\ell = (\hat{\sigma}_x^\ell + i\hat{\sigma}_y^\ell)/2$ ,  $\hat{\sigma}_-^\ell = (\hat{\sigma}_x^\ell - i\hat{\sigma}_y^\ell)/2$ , and  $\hat{B}_r^{(\ell)}$  is the bosonic annihilation operator for the  $r$ th mode of the bath attached at the  $\ell$ th site. Here,  $\omega_0^{(\ell)}$ ,  $g$ , and  $g\Delta$  represent the magnetic field, the overall spin-spin coupling strength, and the anisotropy, respectively. The total number of excitations in the system is given by  $\hat{N}_S = \sum_{\ell=1}^N \hat{\sigma}_+^\ell \hat{\sigma}_-^\ell$  and it satisfies  $[\hat{N}_S, \hat{H}_S] = 0$ . We consider bosonic baths described by Ohmic spectral functions with Gaussian cutoffs,  $\mathfrak{J}_\ell(\omega) = \sum_k 2\pi |\kappa_{\ell k}|^2 \delta(\omega - \Omega_k^\ell) = \omega e^{-(\omega/\omega_c)^2} \Theta(\omega)$ , where  $\Theta(\omega)$  is the Heaviside step function and  $\omega_c$  is the cutoff frequency. The setup is exactly of the form of Fig. 1, with the initial inverse temperatures and chemical potentials of the baths as shown. We look at the equilibrium and nonequilibrium steady states as obtained by RE, LLE, ELE, and ULE. The explicit forms of all these equations for the XXZ spin chain are given in Appen-

dices A, B, C, and D, respectively. For numerical simplicity, we consider the  $N = 3$  case, which is sufficient to demonstrate the fundamental limitations of all three Lindblad equations. All numerical results below are obtained using QUTIP [59,60].

First, we look at the equilibrium case (top row of Fig. 2),  $\beta_L = \beta_R = \beta$ ,  $\mu_L = \mu_R = \mu$ , and calculate the trace distance [46],  $D(\hat{\rho}_{\text{eq}}, \hat{\rho}_{\text{th}}) = \text{Tr}[\sqrt{(\hat{\rho}_{\text{eq}} - \hat{\rho}_{\text{th}})^2}]/2$ , between the steady state  $\hat{\rho}_{\text{eq}}$  given by the three QMEs and the thermal state  $\hat{\rho}_{\text{th}} = \frac{e^{-\beta(\hat{H}_S - \mu \hat{N}_S)}}{\text{Tr}(e^{-\beta(\hat{H}_S - \mu \hat{N}_S)})}$ . The trace distance  $D(\hat{\rho}_{\text{eq}}, \hat{\rho}_{\text{th}})$  is plotted as a function of  $g$  for  $\epsilon = 0.1$  in Fig. 2(a). We see that the trace distance is quite small and of the same order for RE and ULE, and does not vary much with  $g$ . On the other hand, the trace distance for LLE is larger and grows with  $g$ , while that for ELE is identically zero. Note that generically any system is expected to have steady-state coherences in the energy eigenbasis in equilibrium [58,61] for any finite  $\epsilon$  and convergence to  $\hat{\rho}_{\text{th}}$  is physically only expected for  $\epsilon \rightarrow 0$ . Nevertheless, as shown in Fig. 2(b), observables such as local magnetizations  $\langle \hat{\sigma}_z^\ell \rangle$ , obtained from ULE and RE, show a very small difference from the thermal expectation values since they depend on populations in leading order.

The same is not true for the spin currents. The bond spin currents in the system  $I_j$  are defined from the continuity equation  $\frac{d\langle \hat{\sigma}_z^j \rangle}{dt} = -i \langle [\hat{\sigma}_z^j, \hat{H}_S] \rangle = I_j - I_{j-1}$ , which gives  $I_j = 4ig(\langle \hat{\sigma}_+^j \hat{\sigma}_-^{j+1} \rangle - \langle \hat{\sigma}_-^j \hat{\sigma}_+^{j+1} \rangle)$ . On the other hand, boundary spin currents are defined by the continuity equation  $\frac{d\langle \hat{M}_z \rangle}{dt} = I_{B_L} + I_{B_R}$ , where  $\hat{M}_z = \sum_{\ell=1}^N \hat{\sigma}_z^\ell$ . For equations of the form given by Eq. (42),  $I_{B_\ell} = \epsilon^2 \text{Tr}(\hat{M}_z \hat{\mathcal{L}}_2^{(\ell)}[\hat{\rho}(t)])$ ,  $\ell = L, R$ , where  $\hat{\mathcal{L}}_2^{(\ell)}$  changes depending on the QME used. In the steady state, local conservation laws require  $I_1 = -I_{B_L} = I_2 = I_{B_R}$ . Further, in equilibrium, currents should be zero [27]. We find that for  $\omega_0^{(1)} \neq \omega_0^{(2)} \neq \omega_0^{(3)}$ , all QMEs except ELE give unphysical currents, even though we have  $\beta_L = \beta_R = \beta$ ,  $\mu_L = \mu_R = \mu$ . However, it is paramount to note that as shown in Fig. 2(c), the currents from RE and the boundary currents from ULE scale as  $\epsilon^4$ , clearly showing that the leading order term  $O(\epsilon^2)$  is zero. This is completely consistent with our discussion in Secs. III D and IV B 3. On the other hand, the bond currents from ULE are different and scale as  $\epsilon^2$ , thereby showing error in leading order and violating local conservation laws. The LLE does not violate local conservation laws, but still gives equilibrium currents scaling as  $\epsilon^2$  [27], thereby showing leading order inaccuracies in both populations and coherences.

Now we discuss the results for the nonequilibrium setup (bottom row of Fig. 2),  $\beta_L \neq \beta_R$ . The currents in NESS as a function of  $g$  are shown in Fig. 2(d). The current from RE matches the boundary current from ULE for all  $g$  and shows a nonmonotonic behavior with  $g$ . On the other hand, LLE fails to capture the nonmonotonicity of the current as a function of  $g$ , and matches only at very small values of  $g$ . The ELE identically gives zero currents inside the system, even in NESS [24]. However, the boundary currents from ELE seem to match reasonably well with RE for sufficiently high  $g$ . Thus, the ELE also violates the local conservation laws in NESS. The local magnetizations in NESS also match from RE and ULE and are significantly different from the LLE and ELE results at high and low  $g$ , respectively, as shown in Fig. 2(e). Finally, in Fig. 2(f), we demonstrate that ULE bond currents

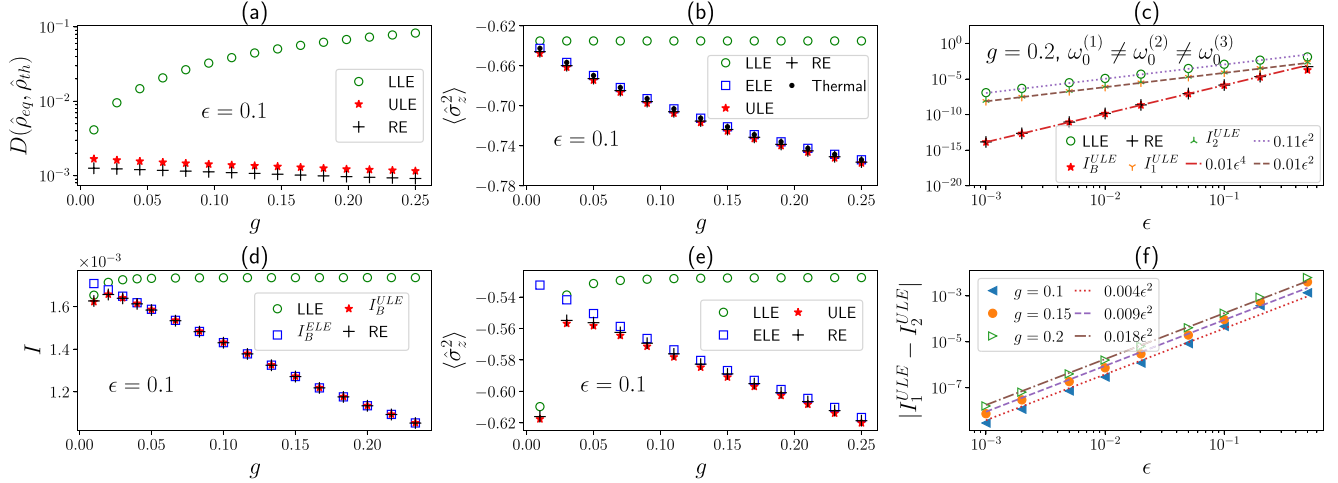


FIG. 2. The top row is for the equilibrium case ( $\beta_L = 1, \beta_R = 1$ ) and the bottom row is for the nonequilibrium case ( $\beta_L = 5, \beta_R = 0.5$ ). Apart from (c), in all other cases,  $\omega_0^{(1)} = \omega_0^{(2)} = \omega_0^{(3)} = 1$ . (a) The trace distance between the expected thermal state  $\hat{\rho}_{\text{th}}$  and the equilibrium steady state  $\hat{\rho}_{\text{eq}}$  as obtained by the LLE, ULE, and RE as a function of  $g$ . (b) The local magnetization in the equilibrium steady state as obtained by LLE, ULE, RE, and ELE and by the expected thermal state as a function of  $g$ . (c) The scaling of spin currents in equilibrium as given by LLE, ULE, and RE as a function of system-bath-coupling strength  $\epsilon$ , for the case where  $\omega_0^{(1)} = 1, \omega_0^{(2)} = 1.5, \omega_0^{(3)} = 2$ . Here,  $I_1^{\text{ULE}}, I_2^{\text{ULE}}$ , and  $I_B^{\text{ULE}}$  refer to the two bond currents and the boundary current as obtained by ULE. (d) Spin currents in NESS as obtained by LLE, ULE, RE, and ELE. For ULE and ELE, only the boundary currents  $I_B^{\text{ULE}}$  and  $I_B^{\text{ELE}}$  are plotted. (For ELE, the bond currents are exactly zero.) (e) The local magnetization in NESS as obtained by LLE, ULE, RE, and ELE as a function of  $g$ . (f) The scaling of the difference between the two bond currents at NESS from ULE as a function of system-bath-coupling strength  $\epsilon$ . Other parameters:  $\mu_L = \mu_R = -0.5, \omega_c = 10$ . All energy parameters are in units of  $\omega_0^{(1)}$ .

are different in NESS with the difference scaling as  $O(\epsilon^2)$ , which highlights a clear violation of local conservation laws in ULE.

All plots in Fig. 2 are made with  $\omega_0^{(1)} = \omega_0^{(2)} = \omega_0^{(3)} = 1$ , except for Fig. 2(c) which was plotted for  $\omega_0^{(1)} = 1, \omega_0^{(2)} = 1.5, \omega_0^{(3)} = 2$ . In Fig. 3, we give the complementary plot,

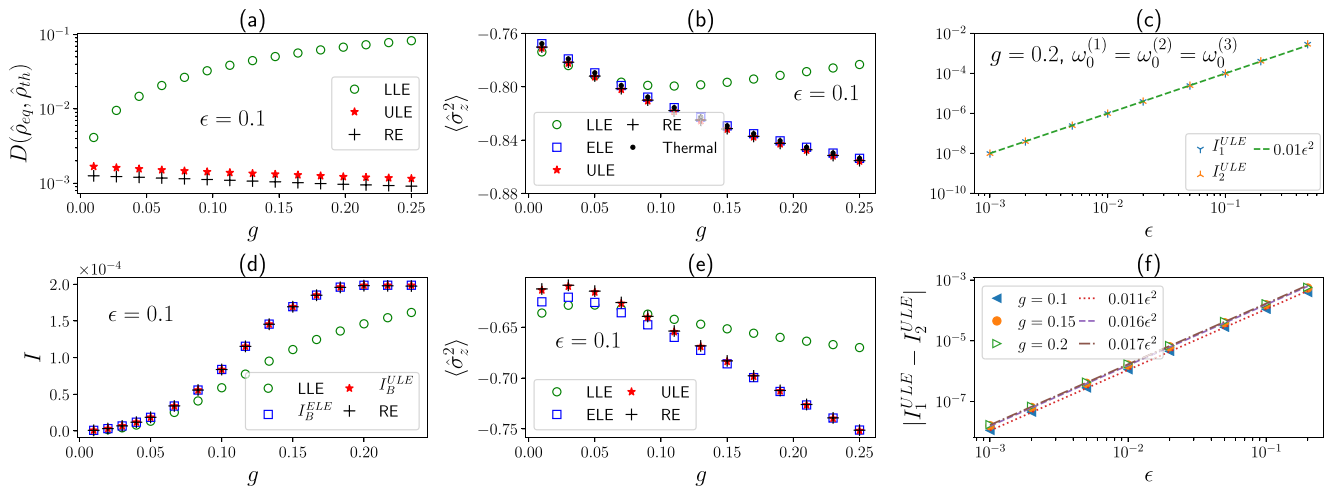


FIG. 3. The top row is for the equilibrium case ( $\beta_L = 1, \beta_R = 1$ ) and the bottom row is for the nonequilibrium case ( $\beta_L = 5, \beta_R = 0.5$ ). Apart from (c), everywhere,  $\omega_0^{(1)} = 1, \omega_0^{(2)} = 1.5, \omega_0^{(3)} = 2$ . (a) The trace distance between the expected thermal state  $\hat{\rho}_{\text{th}}$  and the equilibrium steady state  $\hat{\rho}_{\text{eq}}$  as obtained by the local Lindblad (LLE), universal Lindblad (ULE), and Redfield (RE) equations as a function of  $g$ . (b) The local magnetization in the equilibrium steady state as obtained by LLE, ULE, RE, and ELE and by the expected thermal state as a function of  $g$ . (c) The scaling of bond spin currents in equilibrium as obtained from ULE,  $I_1^{\text{ULE}}, I_2^{\text{ULE}}$ , for the case where  $\omega_0^{(1)} = \omega_0^{(2)} = \omega_0^{(3)} = 1$ . The LLE, RE, and ULE boundary currents are zero correct to numerical precision of  $10^{-16}$ . (d) Spin currents in NESS as obtained by LLE, ULE, RE, and ELE. For ULE and ELE, the boundary currents  $I_B^{\text{ULE}}$  and  $I_B^{\text{ELE}}$  are plotted. (e) The local magnetization in NESS as obtained by LLE, ULE, RE, and ELE as a function of  $g$ . (f) The scaling of the difference between the two bond currents at NESS from ULE as a function of system-bath-coupling strength  $\epsilon$ . Other parameters:  $\mu_1 = \mu_2 = -0.5, \omega_c = 10$ . All energy parameters are in units of  $\omega_0^{(1)}$ .

TABLE II. Accuracy of various QMEs in various settings.

	LLE	ELE	ULE	RE
Diagonal (populations)	O(1) wrong	O(1) wrong in NESS	O(1) correct	O(1) correct
Off-diagonal (coherences)	O( $\epsilon^2$ ) wrong	O( $\epsilon^2$ ) wrong	O( $\epsilon^2$ ) wrong	O( $\epsilon^2$ ) correct
Conservation laws	Conserved	Violated	Violated	Conserved
Thermalization	Violated	Preserved	Preserved	Preserved
Currents from baths	Valid for $g \ll \epsilon$	Valid for $ E_\alpha - E_\gamma  \gg \epsilon$	Valid for all $g$	Valid for all $g$
Currents in system	Valid for $g \ll \epsilon$	Zero	O( $\epsilon^2$ ) wrong	O( $\epsilon^2$ ) correct
Complete positivity	Preserved	Preserved	Preserved	Violated

where all numerical results except Fig. 3(c) are for  $\omega_0^{(1)} = \omega_0^{(2)} = \omega_0^{(3)} = 1$ , while Fig. 3(c) is for  $\omega_0^{(1)} = 1, \omega_0^{(2)} = 1.5, \omega_0^{(3)} = 2$ . Two important things are worth noticing. First, when  $\omega_0^{(1)} = \omega_0^{(2)} = \omega_0^{(3)}$ , none of the LLE, RE, and ULE boundary currents give any unphysical nonzero result (correct to a numerical precision of  $10^{-16}$ ) if  $\beta_L = \beta_R = \beta$ ,  $\mu_L = \mu_R = \mu$ . However, the ULE bond currents still give nonzero  $O(\epsilon^2)$  result and thereby violate local conservation laws. Second, for  $\omega_0^{(1)} = 1, \omega_0^{(2)} = 1.5, \omega_0^{(3)} = 2$ , because of the already large separation between the on-site magnetic fields, the secular approximation performs much better and, as a result, ELE gives reasonably accurate results both in the equilibrium and out-of-equilibrium steady states, for a wide range of  $g$ . However, ELE, by construction, gives zero currents inside the system [24]. Table II summarizes the accuracies and validity regimes of the various QMEs. Although our numerical demonstration is for  $N = 3$ , our analytical understanding in previous sections shows that these issues persist for larger  $N$ , as well as generically for other systems.

## VI. SUMMARY AND DISCUSSIONS

In this work, we have investigated the fundamental limitations of QMEs obtained in the weak system-bath-coupling approach to describe a quantum system coupled to multiple macroscopic baths which can be at different temperatures and chemical potentials, in the absence of any external driving (i.e., when the Hamiltonian is time independent). Microscopically obtaining the QME up to leading order in the system-bath coupling leads to the so-called Redfield form, which is known to generically violate the requirement of complete positivity. Very often, further approximations are done on the Redfield form to reduce it to a Lindblad form, so that complete positivity is restored. We have laid down some fundamental requirements (Table I) that any such approximation must satisfy. If they are violated, there occur physical inconsistencies such as inaccuracies in the leading order populations and coherences in the energy eigenbasis, violation of thermalization when all baths have the same temperatures and chemical potentials, and violation of local conservation laws at NESS. This has allowed us to check for the occurrence of these physical inconsistencies in weak system-bath-coupling QMEs in general, without writing them for any particular model. This model-independent general discussion distinguishes our work from most previous works investigating the accuracies of various QMEs [16,17,23–37].

We have found that the Redfield equation, despite being generically not completely positive, does not violate any of the other fundamental requirements. It therefore gives correct populations and coherences in the energy eigenbasis to the leading order, shows thermalization, and preserves local conservation laws. On the other hand, weak system-bath-coupling Lindblad descriptions violate one or more of the fundamental requirements and thereby have one or more of the physical inconsistencies mentioned above, despite being completely positive. In particular, it can be argued that no existing weak system-bath-coupling Lindblad description, to our knowledge, can generically give both correct populations and correct coherences to the leading order. As an example, we have explicitly shown these violations in generality for the so-called universal Lindblad equation, which has been recently derived. We have also numerically demonstrated these statements in a three-site XXZ chain coupled to two bosonic baths. From our results, it seems that there is no consistent way to correct the violation of complete positivity of the Redfield equation without going to higher orders in system-bath coupling.

These results are extremely significant because weak system-bath-coupling Lindblad equations remain the most widely used descriptions of open quantum systems, and an accurate description of populations, coherences, and currents is important for quantum information and thermodynamics [46–56]. It seems the Redfield equation, despite not being completely positive, should be the description of choice. The various errors in the Redfield equations are controlled. Whether or not a result obtained from the Redfield equation can be trusted can be determined by checking its scaling with system-bath-coupling strength. Further, there have been techniques suggested to infer the next order corrections to populations in a steady state from the Redfield equation without actually writing the next higher-order QME [62–64]. These techniques may be able to correct the positivity issues in the steady state obtained from the Redfield equation [58].

It is paramount to mention that the fundamental limitations of Lindblad descriptions discussed in this paper pertain to the case of a system weakly coupled to multiple thermal baths in the absence of any external driving. In the presence of particular kinds of driving, Lindblad equations can be microscopically derived even for strong system-bath coupling [65]. Our results do not pertain to those descriptions. Further, our results do not pertain to cases where the Lindblad dissipators do not act on the system, but rather on the bath degrees of freedom. Such approaches can be shown to accurately

describe the steady state of the system for arbitrary strength of system-bath coupling [66]. Our results, however, do show that it is imperative to go beyond weak system-bath-coupling QMEs for a physically consistent description of open quantum systems.

### ACKNOWLEDGMENTS

M.K. would like to acknowledge the support from Project No. 6004-1 of the Indo-French Centre for the Promotion of Advanced Research (IFCPAR), Ramanujan Fellowship (SB/S2/RJN-114/2016), SERB Early Career Research Award (Award No. ECR/2018/002085), and SERB Matrics Grant (Grant No. MTR/2019/001101) from the Science and Engineering Research Board (SERB), Department of Science and Technology, Government of India. A.D. and M.K. acknowledge the support of the Department of Atomic Energy, Government of India, under Project No. RTI4001. A.P. acknowledges funding from the European Research Council (ERC) under the European Unions Horizon 2020 research and innovation program (Grant Agreement No. 758403).

### APPENDIX

The example we looked at in the main text is the three-site Heisenberg model, coupled to two different bosonic baths at the first and the third sites. Here, we will give the QMEs used for this setup and write them for a Heisenberg spin chain of length  $N$ .

#### APPENDIX A: REDFIELD EQUATION

The Redfield equation for our setup is given by

$$\begin{aligned} \frac{\partial \hat{\rho}}{\partial t} = & i[\hat{\rho}, \hat{H}_S] \\ & - \epsilon^2 \sum_{\ell=1, N} \sum_{\alpha, \gamma=1}^{2^N} \{ [\hat{\rho} |E_\alpha\rangle \langle E_\alpha| \hat{\sigma}_-^\ell |E_\gamma\rangle \langle E_\gamma|, \hat{\sigma}_+^\ell] C_\ell(\alpha, \gamma) \\ & + [\hat{\sigma}_+^\ell |E_\alpha\rangle \langle E_\alpha| \hat{\sigma}_-^\ell |E_\gamma\rangle \langle E_\gamma| \hat{\rho}] D_\ell(\alpha, \gamma) + \text{H.c.} \}, \end{aligned} \quad (\text{A1})$$

with

$$\begin{aligned} C_\ell(\alpha, \gamma) = & \frac{\tilde{\mathfrak{J}}_\ell(E_{\gamma\alpha}) n_\ell(E_{\gamma\alpha})}{2} - i\text{P} \int_0^\infty d\omega \frac{\tilde{\mathfrak{J}}_\ell(\omega) n_\ell(\omega)}{\omega - E_{\gamma\alpha}}, \\ D_\ell(\alpha, \gamma) = & \frac{e^{\beta\ell(E_{\gamma\alpha} - \mu\epsilon)} \tilde{\mathfrak{J}}_\ell(E_{\gamma\alpha}) n_\ell(E_{\gamma\alpha})}{2} \\ & - i\text{P} \int_0^\infty d\omega \frac{e^{\beta\ell(\omega - \mu\epsilon)} \tilde{\mathfrak{J}}_\ell(\omega) n_\ell(\omega)}{\omega - E_{\gamma\alpha}}, \end{aligned} \quad (\text{A2})$$

where P denotes the Cauchy principal value. Here,  $|E_\alpha\rangle$  and  $|E_\gamma\rangle$  are simultaneous eigenkets of the system Hamiltonian and the magnetization operator, with eigenenergies  $E_\alpha$  and  $E_\gamma$ , where  $E_{\gamma\alpha} = E_\gamma - E_\alpha$ .

#### APPENDIX B: LOCAL LINDBLAD EQUATION

The local Lindblad equation, which can be derived microscopically for  $g \ll \epsilon$ , from the Redfield equation, is given

by

$$\begin{aligned} \frac{\partial \hat{\rho}}{\partial t} = & i[\hat{\rho}, \hat{H} + \hat{H}_{LS}] + \epsilon^2 \sum_{\ell=1, N} \tilde{\mathfrak{J}}_\ell(\omega_0^{(\ell)}) (n_\ell(\omega_0^{(\ell)}) + 1) \\ & \times \left( \hat{\sigma}_-^\ell \hat{\rho} \hat{\sigma}_+^\ell - \frac{1}{2} \{ \hat{\sigma}_+^\ell \hat{\sigma}_-^\ell, \hat{\rho} \} \right) \\ & + \tilde{\mathfrak{J}}_\ell(\omega_0^{(\ell)}) n_\ell(\omega_0^{(\ell)}) \left( \hat{\sigma}_+^\ell \hat{\rho} \hat{\sigma}_-^\ell - \frac{1}{2} \{ \hat{\sigma}_-^\ell \hat{\sigma}_+^\ell, \hat{\rho} \} \right), \end{aligned} \quad (\text{B1})$$

where  $\hat{H}_{LS} = \sum_{\ell=1, N} (\bar{\Delta}_\ell + 2\bar{\Delta}'_\ell) \frac{a_0^{(\ell)}}{2}$ , and  $\bar{\Delta}_\ell$  and  $\bar{\Delta}'_\ell$  are given by

$$\begin{aligned} \bar{\Delta}_\ell = & \text{P} \frac{\epsilon^2}{2\pi} \int_0^\infty d\omega \frac{\tilde{\mathfrak{J}}_\ell(\omega)}{\omega_0^{(\ell)} - \omega}, \\ \bar{\Delta}'_\ell = & \text{P} \frac{\epsilon^2}{2\pi} \int_0^\infty d\omega \frac{\tilde{\mathfrak{J}}_\ell(\omega) n_\ell(\omega)}{\omega_0^{(\ell)} - \omega}. \end{aligned} \quad (\text{B2})$$

#### APPENDIX C: EIGENBASIS LINDBLAD EQUATION

The eigenbasis Lindblad equation is obtained from the Redfield equation by doing the so-called secular approximation [8]. This amounts to an equation of the form

$$\begin{aligned} \frac{\partial \hat{\rho}}{\partial t} = & i[\hat{\rho}, \hat{H}_S] - \epsilon^2 \sum_{\ell=1, N} \sum_{\alpha, \gamma=1}^{2^N} \sum_{\substack{\alpha', \gamma'=1 \\ E_{\gamma'\alpha'}=E_{\gamma\alpha}}}^{2^N} \\ & \{ [\hat{\rho} |E_\alpha\rangle \langle E_\alpha| \hat{\sigma}_-^\ell |E_\gamma\rangle \langle E_\gamma|, |E_{\gamma'}\rangle \langle E_{\gamma'}| \hat{\sigma}_+^\ell |E_{\alpha'}\rangle \langle E_{\alpha'}|] \\ & \times C_\ell(\alpha, \gamma) + [|E_{\gamma'}\rangle \langle E_{\gamma'}| \hat{\sigma}_+^\ell |E_{\alpha'}\rangle \langle E_{\alpha'}|, \\ & |E_\alpha\rangle \langle E_\alpha| \hat{\sigma}_-^\ell |E_\gamma\rangle \langle E_\gamma| \hat{\rho}] D_\ell(\alpha, \gamma) + \text{H.c.} \}, \end{aligned} \quad (\text{C1})$$

where the  $C_l$  and  $D_l$  constants are the same as in Redfield, given by Eq. (A2).

#### APPENDIX D: UNIVERSAL LINDBLAD EQUATION

The universal Lindblad equation for our setup is derived from the steps described in [40]. The ULE equation is then given by

$$\begin{aligned} \frac{\partial \hat{\rho}}{\partial t} = & -i[\hat{H}_S + \hat{H}_{LS}, \hat{\rho}] \\ & + \sum_{\ell, k} \left( \hat{L}_{(\ell, k)} \hat{\rho} \hat{L}_{(\ell, k)}^\dagger - \frac{1}{2} \{ \hat{L}_{(\ell, k)}^\dagger \hat{L}_{(\ell, k)}, \hat{\rho} \} \right). \end{aligned} \quad (\text{D1})$$

The Lamb shift  $\hat{H}_{LS}$  and Lindblad operators  $\hat{L}_{(\ell, k)}$  are given by

$$\begin{aligned} \hat{L}_{(\ell, k)} = & 2\pi\epsilon \sum_{\alpha, \gamma, \ell', k'} \mathbf{g}_{(\ell, \ell', k, k')} (E_{\gamma\alpha}) \mathbf{X}_{\alpha\gamma}^{(\ell', k')} |E_\alpha\rangle \langle E_\gamma|, \\ \hat{H}_{LS} = & \sum_{\alpha\gamma\eta; \ell k \ell' k'} \mathbf{X}_{\alpha\eta}^{(\ell, k)} \mathbf{X}_{\eta\gamma}^{(\ell', k')} \mathbf{f}_{\ell, \ell', k, k'} (E_{\alpha\eta}, E_{\gamma\eta}) |E_\alpha\rangle \langle E_\gamma|, \end{aligned} \quad (\text{D2})$$



where  $X_{\alpha\gamma}^{(\ell,k)} = \langle E_\alpha | \hat{X}_{(\ell,k)} | E_\gamma \rangle$ , and

$$f(p, q) = -2\pi \epsilon^2 \mathcal{P} \int_{-\infty}^{\infty} d\omega \frac{\mathbf{g}(\omega - p)\mathbf{g}(\omega + q)}{\omega}. \quad (\text{D3})$$

Note that  $\mathbf{g}_{(\ell,\ell',k,k')}$  should be treated as a matrix with row index  $(\ell, k)$  and column index  $(\ell', k')$ . Thus,  $[\mathbf{g}(\omega - p)\mathbf{g}(\omega + q)]_{(\ell,\ell',k,k')} = \sum_{(\ell'',k'')} \mathbf{g}(\omega - p)_{(\ell,\ell',k,k')(\ell'',k'')} \mathbf{g}(\omega + q)_{(\ell'',k'')(\ell,\ell',k,k')}$ . The  $\mathbf{g}(\omega)$  matrix captures the effect of the bath on the system, and

can be evaluated to be

$$\mathbf{g}_{(\ell,\ell',k,k')}(\omega) = \delta_{\ell,\ell'} \begin{cases} \frac{\sqrt{3_\ell(-\omega)n_\ell(-\omega)}}{4\sqrt{2\pi}} \begin{pmatrix} 1 & i \\ -i & 1 \end{pmatrix}_{k,k'} & \text{if } \omega < 0, \\ \frac{\sqrt{3_\ell(\omega)(1+n_\ell(\omega))}}{4\sqrt{2\pi}} \begin{pmatrix} 1 & -i \\ i & 1 \end{pmatrix}_{k,k'} & \text{if } \omega > 0. \end{cases} \quad (\text{D4})$$

As in the Redfield case,  $|E_\alpha\rangle$ ,  $|E_\gamma\rangle$  are eigenkets of the system Hamiltonian with eigenenergies  $E_\alpha$  and  $E_\gamma$ , and  $E_{\gamma\alpha} = E_\gamma - E_\alpha$ .

- 
- [1] K. L. Hur, L. Henriët, A. Petrescu, K. Plekhanov, G. Roux, and M. Schiró, *C. R. Phys.* **17**, 808 (2016).
  - [2] *Thermodynamics in the Quantum Regime*, edited by F. Binder, L. A. Correa, C. Gogolin, J. Anders, and G. Adesso (Springer, Cham, 2018).
  - [3] Y. Cao, J. Romero, J. P. Olson, M. Degroote, P. D. Johnson, M. Kieferová, I. D. Kivlichan, T. Menke, B. Peropadre, N. P. D. Sawaya *et al.*, *Chem. Rev.* **119**, 10856 (2019).
  - [4] D. D. Awschalom, C. H. R. Du, R. He, J. Heremans, A. Hoffmann, J. Hou, H. Kurebayashi, Y. Li, L. Liu, V. Novosad, J. Sklenar, S. Sullivan, D. Sun, H. Tang, V. Tyberkevych, C. Trevillian, A. W. Tsen, L. Weiss, W. Zhang, X. Zhang *et al.*, *IEEE Trans. Quantum Eng.* **2**, 1 (2021).
  - [5] J. Cao, R. J. Cogdell, D. F. Coker, H.-G. Duan, J. Hauer, U. Kleinekathöfer, T. L. C. Jansen, T. Mančal, R. J. D. Miller, J. P. Ogilvie, V. I. Prokhorenko, T. Renger, H.-S. Tan, R. Tempelaar, M. Thorwart, E. Thyryhaug, S. Westenhoff, and D. Zigmantas, *Sci. Adv.* **6**, eaaz4888 (2020).
  - [6] V. Gorini, A. Kossakowski, and E. C. G. Sudarshan, *J. Math. Phys.* **17**, 821 (1976).
  - [7] G. Lindblad, *Commun. Math. Phys.* **48**, 119 (1976).
  - [8] H.-P. Breuer and F. Petruccione, *The Theory of Open Quantum Systems* (Oxford University Press, Oxford, 2006).
  - [9] H. Carmichael, *Statistical Methods in Quantum Optics I. Master Equations and Fokker-Planck Equations* (Springer-Verlag, Berlin, 2002).
  - [10] A. Rivas and S. F. Hulega, *Open Quantum Systems* (Springer, Berlin, Heidelberg, 2012).
  - [11] H. Weimer, A. Kshetrimayum, and R. Orús, *Rev. Mod. Phys.* **93**, 015008 (2021).
  - [12] M. B. Plenio and P. L. Knight, *Rev. Mod. Phys.* **70**, 101 (1998).
  - [13] J. Dalibard, Y. Castin, and K. Mølmer, *Phys. Rev. Lett.* **68**, 580 (1992).
  - [14] K. Mølmer, Y. Castin, and J. Dalibard, *J. Opt. Soc. Am. B* **10**, 524 (1993).
  - [15] A. G. Redfield, *Adv. Magn. Reson.* **1**, 1 (1965).
  - [16] R. Hartmann and W. T. Strunz, *Phys. Rev. A* **101**, 012103 (2020).
  - [17] P. R. Eastham, P. Kirton, H. M. Cammack, B. W. Lovett, and J. Keeling, *Phys. Rev. A* **94**, 012110 (2016).
  - [18] S. Anderloni, F. Benatti, and R. Floreanini, *J. Phys. A: Math. Theor.* **40**, 1625 (2007).
  - [19] P. Gaspard and M. Nagaoka, *J. Chem. Phys.* **111**, 5668 (1999).
  - [20] D. Kohen, C. C. Marston, and D. J. Tannor, *J. Chem. Phys.* **107**, 5236 (1997).
  - [21] S. Gnutzmann and F. Haake, *Z. Phys. B* **101**, 263 (1996).
  - [22] A. Suárez, R. Silbey, and I. Oppenheim, *J. Chem. Phys.* **97**, 5101 (1992).
  - [23] D. F. Walls, *Z. Phys.* **234**, 231 (1970).
  - [24] H. Wichterich, M. J. Henrich, H.-P. Breuer, J. Gemmer, and M. Michel, *Phys. Rev. E* **76**, 031115 (2007).
  - [25] Á. Rivas, A. D. K. Plato, S. F. Huelga, and M. B. Plenio, *New J. Phys.* **12**, 113032 (2010).
  - [26] G. Deçordi and A. Vidiella-Barranco, *Opt. Commun.* **387**, 366 (2017).
  - [27] A. Levy and R. Kosloff, *Europhys. Lett.* **107**, 20004 (2014).
  - [28] A. Purkayastha, A. Dhar, and M. Kulkarni, *Phys. Rev. A* **93**, 062114 (2016).
  - [29] A. S. Trushechkin and I. V. Volovich, *Europhys. Lett.* **113**, 30005 (2016).
  - [30] P. P. Hofer, M. Perarnau-Llobet, L. D. M. Miranda, G. Haack, R. Silva, J. B. Brask, and N. Brunner, *New J. Phys.* **19**, 123037 (2017).
  - [31] J. O. González, L. A. Correa, G. Nocerino, J. P. Palao, D. Alonso, and G. Adesso, *Open Syst. Inf. Dynam.* **24**, 1740010 (2017).
  - [32] M. T. Mitchison and M. B. Plenio, *New J. Phys.* **20**, 033005 (2018).
  - [33] M. Cattaneo, G. L. Giorgi, S. Maniscalco, and R. Zambrini, *New J. Phys.* **21**, 113045 (2019).
  - [34] F. Benatti, R. Floreanini, and L. Memarzadeh, *Phys. Rev. A* **102**, 042219 (2020).
  - [35] M. Konopik and E. Lutz, *Phys. Rev. Research* **4**, 013171 (2022).
  - [36] S. Scali, J. Anders, and L. A. Correa, *Quantum* **5**, 451 (2021).
  - [37] F. Benatti, R. Floreanini, and L. Memarzadeh, *PRX Quantum* **2**, 030344 (2021).
  - [38] A. Trushechkin, *Phys. Rev. A* **103**, 062226 (2021).
  - [39] D. Davidovic, arXiv:2112.07863.
  - [40] F. Nathan and M. S. Rudner, *Phys. Rev. B* **102**, 115109 (2020).
  - [41] E. Kleinherbers, N. Szpak, J. König, and R. Schützhold, *Phys. Rev. B* **101**, 125131 (2020).
  - [42] D. Davidović, *Quantum* **4**, 326 (2020).
  - [43] E. Mozgunov and D. Lidar, *Quantum* **4**, 227 (2020).
  - [44] G. McCauley, B. Cruikshank, D. I. Bondar, and K. Jacobs, *npj Quantum Inf.* **6**, 74 (2020).
  - [45] G. Kiršanskas, M. Franckić, and A. Wacker, *Phys. Rev. B* **97**, 035432 (2018).
  - [46] M. A. Nielsen and I. L. Chuang, *Quantum Computation and Quantum Information: 10th Anniversary Edition*, 10th ed. (Cambridge University Press, New York, 2011).
  - [47] C. H. Bennett and D. P. DiVincenzo, *Nature (London)* **404**, 247 (2000).

- [48] A. Streltsov, G. Adesso, and M. B. Plenio, *Rev. Mod. Phys.* **89**, 041003 (2017).
- [49] M. Lostaglio, K. Korzekwa, D. Jennings, and T. Rudolph, *Phys. Rev. X* **5**, 021001 (2015).
- [50] V. Narasimhachar and G. Gour, *Nat. Commun.* **6**, 7689 (2015).
- [51] M. T. Mitchison, M. P. Woods, J. Prior, and M. Huber, *New J. Phys.* **17**, 115013 (2015).
- [52] A. E. Allahverdyan, R. Balian, and T. M. Nieuwenhuizen, *Europhys. Lett.* **67**, 565 (2004).
- [53] K. Korzekwa, M. Lostaglio, J. Oppenheim, and D. Jennings, *New J. Phys.* **18**, 023045 (2016).
- [54] P. Kammerlander and J. Anders, *Sci. Rep.* **6**, 22174 (2016).
- [55] J. P. Santos, L. C. Céleri, G. T. Landi, and M. Paternostro, *npj Quantum Inf.* **5**, 23 (2019).
- [56] G. Francica, J. Goold, and F. Plastina, *Phys. Rev. E* **99**, 042105 (2019).
- [57] C. H. Fleming and N. I. Cummings, *Phys. Rev. E* **83**, 031117 (2011).
- [58] A. Purkayastha, G. Guarnieri, M. T. Mitchison, R. Filip, and J. Goold, *npj Quantum Inf.* **6**, 27 (2020).
- [59] J. Johansson, P. Nation, and F. Nori, *Comput. Phys. Commun.* **183**, 1760 (2012).
- [60] J. Johansson, P. Nation, and F. Nori, *Comput. Phys. Commun.* **184**, 1234 (2013).
- [61] G. Guarnieri, M. Kolář, and R. Filip, *Phys. Rev. Lett.* **121**, 070401 (2018).
- [62] J. Thingna, J.-S. Wang, and P. Hänggi, *J. Chem. Phys.* **136**, 194110 (2012).
- [63] J. Thingna, J.-S. Wang, and P. Hänggi, *Phys. Rev. E* **88**, 052127 (2013).
- [64] X. Xu, J. Thingna, and J.-S. Wang, *Phys. Rev. B* **95**, 035428 (2017).
- [65] M. Cattaneo, G. De Chiara, S. Maniscalco, R. Zambrini, and G. L. Giorgi, *Phys. Rev. Lett.* **126**, 130403 (2021).
- [66] M. Brenes, J. J. Mendoza-Arenas, A. Purkayastha, M. T. Mitchison, S. R. Clark, and J. Goold, *Phys. Rev. X* **10**, 031040 (2020).